Journal of Thermal Analysis, Vol. 48 (1997) 1273-1282

INFLUENCE OF HEAT SOURCE DISTRIBUTIONS IN GaAs/GaAlAs QUANTUM-WELL HIGH-POWER LASER ARRAYS ON TEMPERATURE PROFILE AND THERMAL RESISTANCE

R. Puchert, U. Menzel, A. Bärwolff, M. Voß, and Ch. Lier

Max-Born-Institut für Nichtlineare Optik und Kurzzeitspektroskopie, Rudower Chaussee 6, D–12489 Berlin, Germany

(Received April 19, 1996; in revised form January 8, 1997)

Abstract

The thermal behaviour of high-power GaAlAs/GaAs laser arrays is described by a comprehensive thermal two-dimensional finite-element model which takes several heat sources into account. The influence of these different heat sources on the two-dimensional temperature distribution in the laser array has been investigated. The power densities of the heat sources related to the active region were calculated by an analytic description of the temperature dependent processes as spontaneous emission, Auger recombination and interface recombination. The results of our numerical calculation show, that the local distribution of the heat sources has a strong influence on the lateral temperature profile and on the maximum temperature in the active region of the array, i.e. on the thermal resistance. The calculated temperature profiles are in a good agreement with the measured lateral temperatures at different injection currents and heat sink temperatures. The difference between calculated and measured maximum temperature is lower than 0.75°C.

Keywords: finite element method, semiconductor laser, temperature distribution

Introduction

High-power semiconductor laser diodes and arrays are efficient devices to pump solid state lasers [1, 2]. In spite of high electrical-to-optical conversion efficiency (about 50–60%) and effective thermal mounting of the devices to a heat sink, a large amount of loss power leads to a considerable increase of temperature in the active zone of the laser diode under high-power operation. As a result, the threshold current shifts to higher values, the output power and the efficiency are reduced due to increasing nonradiative recombination, the emission wavelength shifts to longer wavelength, and the degradation process is accelerated [3].

Therefore, many theoretical and experimental investigations have been performed to improve the thermal properties of laser diodes, including the mounting with efficient heat removals [4–6]. Nevertheless, at high output powers a tempera-

0368–4466/97/ $ 5.00

John Wiley & Sons Limited
Chichester

ture rise ΔT in the diode occurs, which in the simplest approximation can be estimated from the thermal resistance R_{Th}

$$R_{Th} = \frac{\Delta T}{P_L} \tag{1}$$

where P_L is the loss power.

In most cases, the maximum temperature occurs in the centre of the emitting area. In multistripe arrays, also a lateral temperature variation between the single emitters occurs, because the heat sources are distributed along this direction [7].

In order to predict the thermal behaviour of the laser arrays it is necessary to study the influence of the heat sources under high power conditions. In this paper, the temperature profile in a GaAs/GaAlAs laser array is calculated under consideration of several loss processes and their different spatial distribution inside the semiconductor laser chip. The power densities of the temperature-dependent heat sources are calculated by using a model described in [8]. This model gives the contribution of spontaneous emission, Auger and interface recombination to the total loss power at a specific temperature. However, the different loss processes are located in different regions of the structure. We present results which show the influence of the strength and the localisation of the loss processes on the two-dimensional temperature distribution and on the thermal resistance.

Laser structure

A simplified scheme of the investigated DQW GaAs/GaAlAs 20-stripe laser array is depicted in Fig. 1. The array emits at a wavelength of 810 nm. Each single emitter has a stripe width of about 4 μm, the distance between the emitters is 6 μm. The chip has a width of 400 μm, a resonator length of 600 μm and is mounted on a copper heat sink which is placed on a Peltier cooled stage. The temperature is sta-

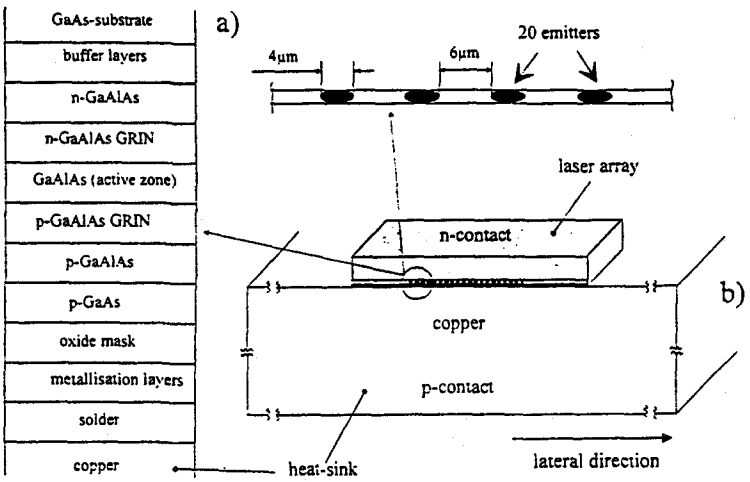

Fig. 1 Scheme of the laser diode structure (a) and the laser chip mounted on a heat sink (b)

Table 1 Resistances of the layers being the main sources for Joule heating

Layer	Resistance/mΩ
p-contact	41.6
p-GaAs	1.125
p-GaAlAs	43.35
n-GaAs (substrate)	16.8
n-contact	2.08

bilised by a Peltier cooler with an accuracy of 0.1 °C. Our measurements were done under variation of the heat sink temperature in the range of 15–35 °C. The electrical resistances of the layers are given in Table 1. These values have been calculated based on typical electrical resistivities for the given material and doping level. The electrical resistances and the current densities determine the amount of Joule losses within the individual layers. For each active stripe the same current density was used. The layers not listed in Table 1 have negligible electrical resistances and are omitted therefore. The electrical resistances of the GaAlAs GRIN (graded index) layers are averaged values. In our calculation, the multicomponent metallisation layers, as well as the active region (consisting of the wells and the barriers) are treated as a whole with respect to heat conduction. Again, we assign average thermal conductivities to both layers. The thickness and the thermal conductivities of the individual layers are given in Table 2.

Analysis of the heat sources

Under steady-state conditions the heat flow in the laser array is governed by the two-dimensional stationary heat conduction equation

Table 2 Thickness and heat conductivity for the layers used in the FEM calculation

Layer composition	Layer thickness/μm	Heat conductivity/W (m K)$^{-1}$
Copper heat sink	6000	384
Solder	12.0	25.5
Metallisation layers	0.3	144.0
Oxide mask	0.1	8.0
p-GaAs	0.2	44.0
p-GaAlAs	1.5	11.4
p-GaAlAs GRIN	0.23	11.78
GaAlAs, active zone	0.03	22.8
n-GaAlAs GRIN	0.23	11.78
n-GaAlAs	1.7	11.4
buffer layers	0.65	12.0
GaAs-substrate	90.0	44.0

$$\nabla[\lambda(x,y)\nabla T(x,y)] = -q(x,y) \quad (2)$$

where $T(x,y)$ is the lateral temperature distribution [K], $\lambda(x,y)$ is the thermal conductivity of the materials used in the device [W (m K)$^{-1}$], and $q(x,y)$ describes the inhomogeneous distribution of power density of heat production [W m^{-3}]. In contrast to early publications [9] we do not assume that these heat sources are entirely concentrated within the active regions of the multilayer structure. The temperature distribution into the longitudinal (z-) direction is assumed to be homogeneous because the extent of our structure into this direction is much more bigger than the relevant lateral dimensions of the laser array. Thereby effects of facet heating by surface recombination are vanished. As motivated below, the latter mechanism has a minor influence on the overall resonator temperature.

The boundary conditions used in the calculations are:

a) At the upper and at the sideward surfaces of our rectangular structure (Fig. 1) we assume heat convection to air of constant temperature (25°C). The convection coefficient is taken as 25 W K^{-1} m^{-2}.

b) The bottom surface of the heat sink has a fixed temperature of 25°C. This is motivated by the use of the Peltier cooler.

Furthermore, we vanished the temperature dependence of the thermal conductivity because of its small change in the temperature range treated within this paper.

In general, heat generation in a laser diode occurs by non-radiative recombination processes, absorption of light and Joule heating. A detailed analysis of heat sources requires the knowledge of the spatial distribution of the different loss processes in the laser array [10]. From the measured power-current and voltage-current characteristics (Fig. 2) the total loss power, P_L, of the laser array for different heat-

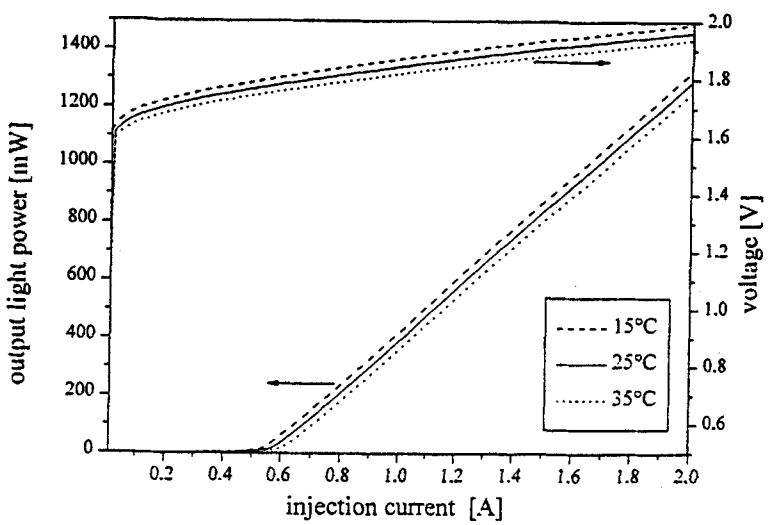

Fig. 2 Power-current (left) and voltage-current characteristics (right) of a 20-stripe GaAlAs DQW laser array at heat sink temperatures of 15, 25 and 35°C

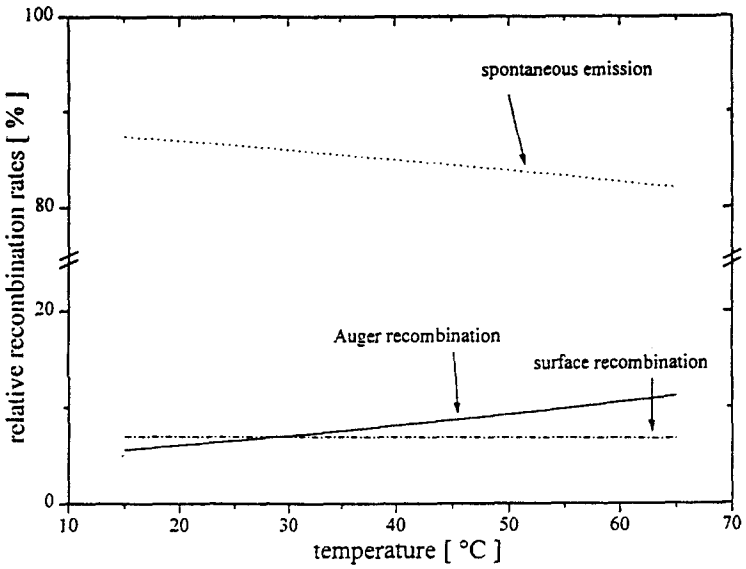

Fig. 3 Temperature dependence of relative recombination rates of Auger and surface recombination and spontaneous emission calculated with the model given in [8]

sink temperatures, T_{HS}, can be determined. The loss power, P_L, consists of (i) Joule heating, P_j, and (ii) losses associated with recombination phenomena in and around the *pn*- junction, P_{pn}. Loss processes at the *pn*-junction are radiative spontaneous emission, interface recombination, Auger recombination, and leakage current. The temperature dependence of these different recombination processes has been calculated using a rate equation model described in [8]. This model is based on a microscopic description of gain and radiative recombination, and on a phenomenological description of interface- and Auger recombination. Using this model, the temperature dependent relative rates of the individual recombination processes (Fig. 3) give the amount of power for the individual process. These loss processes depend on the injection current and on the temperature in the active zone.

The model of thermal behaviour of laser diodes by Joyce and Dixon [9] assumes that heat is generated exclusively in the active zone. In fact, Auger- and interface recombination produce heat only within the active region. Therefore, in our calculation, heat sources arising from Auger- and interface recombination are concentrated to the quantum wells and the barriers, with a lateral extension corresponding to the width of the stripes. In contrast, the spontaneously emitted photons, which have the highest relative recombination rate (Fig. 3) in the considered temperature range, pass the surrounding GaAlAs layers, which have a higher bandgap than the active region. The emitted photons are absorbed far from the active region, in the *n*-doped buffer layers, in the *n*-substrate, in the *p*-doped region, in the GaAs caplayer and in the metallisation layer. To obtain the amount of energy produced within these layers by absorbing spontaneously emitted photons, we took into account the

thickness and the absorption coefficient of these layers. The absorption coefficient of GaAs is approximately $1 \cdot 10^4$ cm^{-1} at the emission wavelength of 810 nm [11]. This gives an absorption length of about 1 μm, respectively the volume in which the photons are absorbed. Further we assume, that the spontaneous emission is isotropic, i.e. the same number of photons are consumed in the *n*-doped and the *p*-doped region. In the *n*-region, the spontaneous emission is absorbed in buffer layers and in the substrate over a length of 1 μm. In the *p*-side region, 10% of the photons are absorbed in the *p*-GaAs cup layer and 40% are absorbed in the metallisation layers with a penetration depth of 0.1 μm. Joule heating occurs in all layers of the diode. If the electrical resistance of a layer is very low, Joule heating is negligible for this layer.

Nonradiative surface recombination occurs only at the facets and leads to a strong temperature rise at the laser mirrors. However, this process is restricted to a very thin region at the facets (some μm). It does not affect the average temperature within the resonator, and has a negligible influence on electrical and optical properties of the device. Therefore, surface recombination is neglected in the current calculation.

Finite element calculation and comparison with experimental data

The finite element method [12] is a powerful numerical tool to solve several thermal problems associated with heat dissipation processes in laser diodes and laser arrays [7, 13, 14]. In the first step the geometry of the laser array is descritized into finite elements for constructing an approximated solution of such thermal problem with boundary condition. In the 1-D case a line element is represented by the thermal resistance R_{Th} between two nodes of the line element:

$$R_{Th} = \frac{L}{\lambda A} \tag{3}$$

where L is the distance [m] and A is the effective cross-sectional area for heat flow between the nodes [m^2]. The heat flux Q between the nodes N1 and N2 can be determined by formula

$$Q(\mathrm{N1} \rightarrow \mathrm{N2}) = \frac{T(\mathrm{N1}) - T(\mathrm{N2})}{R_{Th}(\mathrm{N1} - \mathrm{N2})} \tag{4}$$

where T(N1), T(N2) are the temperatures of nodes. In the 2-D and 3-D case the heat conduction problem consist of a network of such resistors going from node to node in two or three dimensions. Each element can coupled with different material properties (including the thermal conductivity as tensor), representing the layered structure of the laser arrays. Heatsource density profiles characterising the heat generation inside the laser array can associated with these elements. The temperature distribution is defined by a set of polynomials over each element [12]. The spatial variation of the temperature $T(x,y)$ is expressed of n nodal temperatures (n is the

total number of nodes in the model) and an interpolation matrix. The matrix equation in Galerkin formulation [12] is

$$[K]\{T\} = \{Q\} \tag{5}$$

where $\{T\}$ is the unknown matrix representing the temperatures of all nodes. The matrix $[K]$ may be evaluated by summing contribution from all the contributing elements, representing the laser structure. Summing is carried out over each element and over all elements of the full structure under restriction of the boundary conditions. The heat source matrix $\{Q\}$ is also evaluated by summing the heat sources over each element.

We carried out FEM-calculations using the commercial program PATRAN 3 [15]. In the calculations, the FEM-grid was adapted to the geometry of the structure by using appropriate element sizes and shapes. To have sufficient spatial resolution within the active region, we chose rectangular elements – the smallest in our calculation – with a size of 1 μm×0.03 μm there. For the *n*-GaAlAs gradient layers, the *n*-GaAlAs-layer, the solder, and the heat sink we use triangular elements. These elements are suitable to connect the fine grid within the active region with the coarse grid in the other regions. In that way, the numerical stability is increased. The whole grid contains 13210 nodes associated with 21667 elements.

In Fig. 4, the calculated lateral temperature distributions in the laser array across the emitting areas for different injection currents are depicted. The temperature profiles for two heat source distributions are shown. The dashed curves show the calculated temperature profile under the assumption, that all heat sources – besides Joule heating – are concentrated within the active region. In contrast, the straight lines show the calculated profiles for the above described distribution of the heat sources. As can be seen, such distribution of the heat sources leads to a lower modulation of the temperature profile and to a lower maximum temperature. It is indicated that absorption of the spontaneously emitted photons is mainly responsible for the temperature distribution in the laser array. As an example at an injection current of 2 A (heat sink temperature: 25°C) the calculated maximum is 45.6°C. The modulation depth of temperature in the centre of the active region is merely 0.5°C. If the loss power P_{pn} is only concentrated in the active region these values increase to 48.4 and 2.5°C, respectively. These results indicate the influence of the loss power density in the active region on the maximum temperature determined by the geometry of the emitting stripes and the amount of loss power. Nevertheless the spatial distribution of the absorbed spontaneous emission and the distance between the stripes influence the temperature distribution in the active region. Calculations with distributed heat sources, different stripe width and distance between stripes show, that at a same loss power (I=2 A) the maximum and modulation depth of the temperature decrease from 46.6 and 0.9°C (stripe width: 2 μm stripe, distance between stripes: 8 μm) to 46.1 and 0.3°C (stripe width: 8 μm stripe, distance between stripes: 2 μm) due to the decrease of loss power density.

In contrast the influence of the spatial distribution of the heat sources on the temperature at the edges of the device is small. Because of the high thermal con-

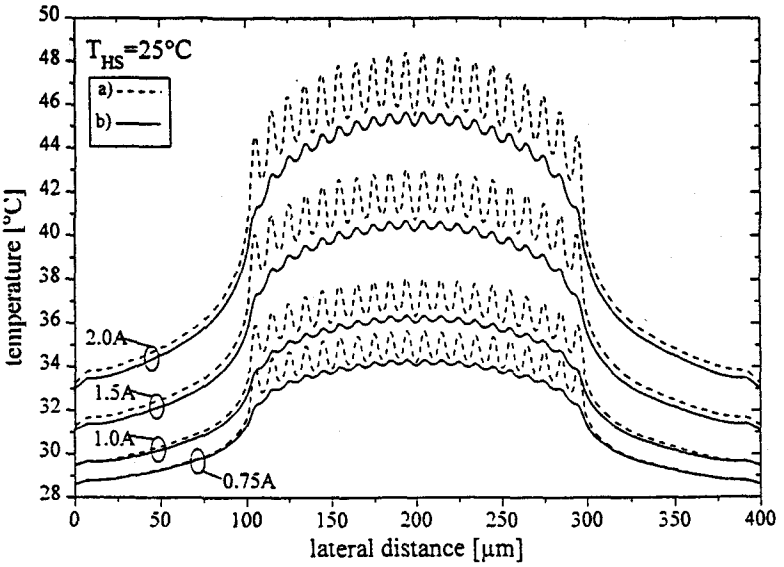

Fig. 4 Calculated lateral temperature distribution in a 20-stripe laser array at four different injection currents; a) *pn* junction losses concentrated within the active region only, b) *pn* junction losses with distributed heat sources

ductivity of the heat sink the heat conduction is much more better in vertical than in lateral direction. This leads to small temperature gradients and heat fluxes in lateral direction. Because of the small heat fluxes in lateral direction heat transfer from the edges via convection is negligible. Calculations with different convective coefficients (ambient and heat sink temperature: 25°C) show temperature changes smaller than 0.1°C. We conclude that the temperature rise at the edges of the device is mainly influenced by the total loss power, the thermal conductivity of the heat sink and the thermal conductivities of the semiconductor layers in the region without emitting stripes. For the same device structure but different heat source distribution a comparable shape of envelope of temperature distribution in the active region is observed. For instance the temperature difference between the outer and centre emitting stripes is 4.3°C with distributed and 3.8°C with concentrated heat sources. The envelopes are primarily different in maximum and modulation depth of temperature in the region of emitting stripes.

A comparison of the computed and measured maximum values of the temperature in the active zone for a single stripe in the centre of the array is depicted in Fig. 5 (heat sink temperature 15 to 35°C). The temperature measurement based on temperature dependent wavelength shifts of the emission spectra [16]. It is shown, that our calculated maximum temperatures reproduce the measured data very well. The difference between measured and calculated maximum temperatures is lower than 0.75°C. For all used heat sink temperatures, the maximum temperature vary linearly with the pumping current.

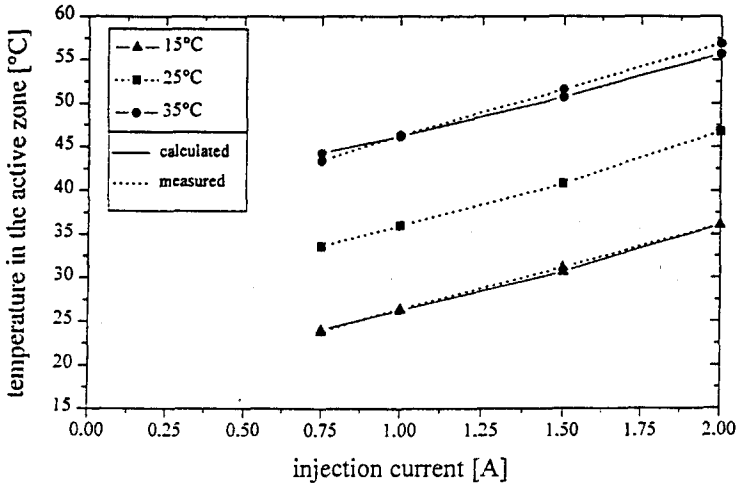

Fig. 5 Calculated and measured maximum temperature in the active region of the centre emitter in a 20-stripe GaAs/GaAlAs laser array, as a function of injection current for three different heat sink temperatures; dashed line – experimental values (wavelength measurements)

For the GaAs/GaAlAs laser array we calculate a thermal resistance of about 7.89 K W^{-1} at an injection current of 1 A. This value is not strong influenced by heat sink temperature (0.1 K W^{-1} per 10°C) in the investigated temperature region. The measured thermal resistance is 7.86 K W^{-1} at a current of 1 A but varies slightly more with heat sink temperature (0.2 K W^{-1} per 10°C). Within the region of low injection current ($I < 1$ A) the difference between measured and calculated values is about 0.7 K W^{-1}. The difference becomes smaller with higher currents. A reason for the difference between measured and calculated values in the lower injection current region, seems to be in the temperature measurement near threshold current (threshold current of the laser array ~500 mA). On the other hand, this result shows, that the magnitude of the thermal resistance is very sensitive to temperature variation for the analysed laser array.

Conclusion

We used a finite element model with spatial distributed heat sources for the calculations of the two dimensional temperature distribution in a high-power laser array. As relevant loss mechanisms in the considered temperature range, we involved radiative spontaneous emission, Auger recombination, interface recombination, and Joule heating. The contribution of the individual loss processes to the total loss, dissipated as heat, is derived from a rate equation model. According to their physical nature, the power densities of heat production are distributed over the structure. We show, that the heat source distribution used in the present finite-element calculation leads to a good agreement with experimental obtained temperatures, in par-

ticular for the more sophisticated structure of the laser array. For distributed heat sources the calculated peak and the modulation depth of the temperature between emitting stripes are lower than using a concentrated heat source in the active region.

* * *

The authors would like to thank Prof. T. Elsaesser for helpful discussion. This work has been supported by Bundesministerium für Bildung, Wissenschaft, Forschung und Technologie (BMBF) under the contract number 13 N6410.

References

1 J. G. Endriz, M. Vakili, G. S. Bowder, M. De Vito, J. M. Haden, G. L. Harnagel, W. L. Plano, M. Sakamoto, D. F. Welch, St. Willing, D. P. Vorland and H.C. Yao, IEEE J. Quantum Electron. QE-28 (1992) 952.
2 M. Sakamoto, J. G. Endriz and D. R. Scifres, Electron. Lett., 28 (1989) 178.
3 M. Sakamoto, D. F. Welch, H. Yao, J. D. Endriz and D. R. Scifres, Electron. Lett., 26 (1990) 729.
4 M. Osinski and W. Nakwaski, Electron. Lett., 29 (1993) 11, 1015.
5 B. M. A. Rahman, S. P. Lepkowski and K. T. V. Grattan, IEE Proc. Optoelecton. Vol. 142, 1995 p. 2, 82.
6 M. Ito and T. Kimura, IEEE J. Quantum Electron. QE-17 (1981) 787.
7 A. Bärwolff, R. Puchert, P. Enders, U. Menzel and D. Ackermann, J. Thermal Anal., 45 (1995) 417.
8 U. Menzel, A. Bärwolff, P. Enders, D. Ackermann, R. Puchert and M. Voss, Semicond. Sci. Technol., 10 (1995) 1382.
9 W. B. Joyce and R. W. Dixon, J. Appl. Physics, 46 (1975) 855.
10 T. Kobayashi and Y. Furukawa, Jap. J. Appl. Phys., 14 (1975) 1981.
11 Landolt-Börnstein, Zahlenwerte und Funktionen aus Naturwissenschaft und Technik, Band 17, Halbleiter, Springer-Verlag Berlin-Heidelberg, 1982.
12 K. H. Huebner and E. A. Thornton, The finite element method for engineers, John Wiley, New York, 1982.
13 R. P. Sarzala and W. Nakwaski, J. Thermal Anal., 36 (1990) 171.
14 R. P. Sarzala and W. Nakwaski, J. Thermal Anal., 39 (1993) 1297.
15 PATRAN 3 is a registered trademark of The MacNeal-Schwendler Corporation.
16 M. Voą, Ch. Lier, A. Bärwolff and T. Elsaesser J. Appl. Phys., 79 (1996) 1170.